Contribution from the University of Utah Medical Center, Salt Lake City, Utah 84132

Characterization of Peptide-Coated Cadmium-Sulfide Crystallites

Charles T. Dameron and Dennis R. Winge*

Received June 23, 1989

Glutathione-related isopeptides of general structure (γ-Glu-Cys)$_n$-Gly, (γEC)$_n$G), serve as a matrix for formation of nanometer-sized cadmium-sulfide crystallites in cultures of *Schizosaccharomyces pombe* and *Candida glabrata* and in vitro. The formation of these complexes constitute a cadmium detoxification response in these organisms. Crystallites formed in vivo and in vitro exhibit numerous properties analogous to quantum semiconductor clusters including luminescence and the ability to mediate the photoreduction of methyl viologen. The (γEC)$_n$G peptides stabilize discrete sizes of the particles against accretion. Isopeptides from (γEC)$_2$G to (γEC)$_4$G preferentially stabilize CdS clusters having band gap transitions indicative of a lattice diameter near 20 Å. Accretion can be facilitated in all clusters at elevated temperatures, acidic pH, or in the presence of free sulfide ions. However, particle coalescence is more facile in clusters containing isopeptides with only two dipeptide repeats (n = 2 peptides). The in vitro formation of CdS crystallites is also dependent on peptide length. Cd(II)-peptide complexes with a greater number of dipeptide repeats are an inferior matrix for crystallite formation. Cysteinyl peptides with α-peptide bonds bind Cd(II) ions and serve as effective matrices for CdS mineralization, but the resulting crystallites exhibit band gap transitions of higher energy than the transitions observed in γ-peptide coated particles.

Introduction

Two classes of molecules function in the detoxification of metal ions such as copper and cadmium in eukaryotic organisms. One is the class of cysteine-rich polypeptides termed metallothioneins.[1,2] Metallothioneins function in metal ion detoxification, but may also have other physiological functions.[3] The second class is a family of peptides related to glutathione (γ-Glu-Cys-Gly) but containing multiple γ-Glu-Cys dipeptide units. The structure (γ-Glu-Cys)$_n$-Gly designated (γEC)$_n$G or γEC peptide contains an isopeptide bond between the γ-carboxyl group of glutamate and the α-amino function of cysteine within the repeat unit. These peptides occur in plants, fungi, and protista under various names, including cadystin and phytochelatin.[4-8] Typically, a heterogeneous mixture of (γEC)$_n$G peptides varying from n = 2 to n = 5 (n specifies the number of dipeptide repeats) is synthesized in response to metal salts.[4,9,10] DesGly variants of the peptides are also evident in plants and fungi.[11,12] The γEC peptides bind metal ions in a metal-cysteinyl thiolate cluster composed of multiple peptides heterogenous in length and metal ions.[8] Metal complex formation is not dependent on length variation as peptides of unique length are capable of binding Cu(I) in specific complexes.[11]

Acid labile sulfide is an additional component of Cd-γEC peptide complexes from plants and fungi but not copper-γEC peptide complexes in *Schizosaccharomyces pombe*.[4,13] Cadmium promotes the incorporation of sulfide into the Cd-peptide clusters by stimulating the synthesis of sulfide.[8,14] The significance of sulfide in metal ion detoxification is substantiated by the isolation of cadmium-hypersensitive mutants in *S. pombe* that produce only sulfide-deficient Cd-γEC peptide complexes.[15] The content of bound sulfide ions in the metal complexes varies depending upon the extent of the sulfide response. Native isolates of the Cd-γEC peptide complex of *Candida glabrata* typically contain a molar sulfide:cadmium ratio between 0.3 and 0.7. Complexes with a S:Cd ratio of 0.7 contain a 20-Å-diameter CdS crystallite coated with the γEC peptides.[16] The crystallites are quantum particles exhibiting size-dependent electronic states, a situation first observed in small synthetic CdS semiconductor particles.[17,18] CdS complexes having lattice sizes in excess of 100 Å in diameter exhibit size-independent spectral transitions.[19]

The intent of the present study was to evaluate native CdS complexes coated with different γEC peptides and to determine if analogous CdS particles form in vitro. We report properties of the quantum particles and evidence that cadmium-sulfide complexes readily form in vitro by the addition of sulfide ions to Cd-γEC peptide complexes. Studies are presented focusing on the influence of the peptide coating on CdS crystallite growth in vitro. Cysteinyl peptides varying in sequence, length, and peptide linkage have been evaluated.

* To whom correspondence should be addressed.

Experimental Section

Preparation of Native CdS Crystallites. Cadmium-peptide complexes were purified from *C. glabrata* (strain ATCC 2001) and *S. pombe* (strain ATCC L972 h-) grown in minimal media containing cadmium salts as reported previously.[8,20]

Preparation of Peptides. γEC peptides of n = 2 type were isolated from *C. glabrata* CdS complexes. Pure Cd-γEC peptide complexes were acidified and chromatographed on a C_8 reverse-phase HPLC column equilibrated in 0.1% trifluoroacetic acid (TFA). Metal-free peptides were resolved with a 0-60% linear acetonitrile gradient and were stored anaerobically in acid (pH 2) at -70 °C.

Large quantities of γEC peptides of n = 2-4 types and of the n = 4 α-analogue were prepared by chemical synthesis according to a manual Merrifield procedure.[21] The starting resin was *t*-Boc-glycyl-derivatized chloromethylated polystyrene (Vega). Synthesis was carried out with *N*-α-*t*-Boc-cysteine (*S*-*p*-methoxybenzyl, Bachem) and *N*-α-*t*-Boc-glutamic acid (Bachem) with either the α- or γ-carboxyl groups protected as the benzyl ester. Coupling efficiency was verified by the ninhydrin method.[22] Trifluoroacetic acid was used to deblock the α-amino *t*-Boc

(1) Hamer, D. H. *Annu. Rev. Biochem.* **1986**, *55*, 913.
(2) Kagi, J. H. R.; Kojima, Y. *Experientia, Suppl.* **1987**, *52*, 25.
(3) Bremner, I. *Experientia, Suppl.* **1987**, *52*, 81.
(4) Hayashi, Y.; Nakagawa, C. W.; Murasugi, A. *EHP, Environ. Health Perspect.* **1986**, *65*, 13.
(5) Grill, E.; Winnacker, E. L.; Zenk, M. H. *Science* **1985**, *230*, 674.
(6) Steffens, J. C.; Hunt, D. F.; Williams, B. G. *J. Biol. Chem.* **1986**, *261*, 13879.
(7) Weber, D. N.; Shaw, C. F., III; Petering, D. H. *J. Biol. Chem.* **1987**, *262*, 6962.
(8) Reese, R. N.; Mehra, R. K.; Tarbet, E. B.; Winge, D. R. *J. Biol. Chem.* **1988**, *263*, 4186.
(9) Hayashi, Y.; Nakagawa, C. W.; Uyakul, D.; Imai, K.; Isobe, M.; Goto, T. *Biochem. Cell Biol.* **1988**, *66*, 288.
(10) Grill, E.; Winnacker, E. L.; Zenk, M. H. *FEBS Lett.* **1986**, *197*, 115.
(11) Mehra, R. K.; Winge, D. R. *Arch. Biochem. Biophys.* **1988**, *265*, 381.
(12) Bernhard, W. R.; Kagi, J. H. R. *Experentia, Suppl.* **1987**, *52*, 309.
(13) Reese, R. N.; Winge, D. R. *J. Biol. Chem.* **1988**, *263*, 12832.
(14) Murasugi, A.; Wada-Nakagawa, C.; Hayashi, Y. *J. Biochem.* **1984**, *96*, 1375.
(15) Mutch, N.; Hayashi, Y. *Biochem. Biophys. Res. Commun.* **1988**, *151*, 32.
(16) Dameron, C. T.; Reese, R. N.; Mehra, R. K.; Kortan, A. R.; Carroll, P. J.; Steigerwald, M. L.; Brus, L. E.; Winge, D. R. *Nature* **1989**, *338*, 596.
(17) Rossetti, R.; Ellison, J. L.; Gibson, J. M.; Brus, L. E. *J. Chem. Phys.* **1984**, *80*, 4464.
(18) Nozik, A. J.; Williams, F.; Nenadovic, M. T.; Rajh, T.; Micic, O. I. *J. Phys. Chem.* **1985**, *89*, 397.
(19) Brus, L. E. *J. Phys. Chem.* **1986**, *90*, 2555.
(20) Mehra, R. K.; Tarbet, E. B.; Gray, W. R.; Winge, D. R. *Proc. Natl. Acad. Sci. U.S.A.* **1985**, *85*, 8815.
(21) Merrifield, R. B. *J. Am. Chem. Soc.* **1963**, *85*, 2149.

0020-1669/90/1329-1343$02.50/0

group. Peptides were cleaved from the resin and side chains deprotected with anhydrous HF in the presence of anisole and β-mercaptoethanol. The synthetic peptides were purified by LH-20 gel (Pharmacia) filtration followed by preparative C_{18} reverse-phase HPLC in 0.1% TFA and a linear gradient of acetonitrile. The peptides were reduced with β-mercaptoethanol at pH 8.6 followed by acidification and chromatography on a semipreparative C_8 reverse-phase HPLC column (Vydac).

The mouse metallothionein hexapeptide fragment of sequence Lys-Cys-Thr-Cys-Cys-Ala was purchased from Sigma Chemical Co. The peptide was reduced and chromatographed on a C_8 reverse-phase HPLC column prior to use. The recovered peptide was quantified by dithiodipyridine titration and amino acid analysis.

Characterization of Peptides. The final step in the purification of each peptide was C_8 reverse-phase HPLC. The acetonitrile concentrations effective in the elution of the n = 2–4 γEC peptides, n = 4 αEC peptide, and the MT hexapeptide were 16.8, 20.4, 24.6, 21.6, and 27.6 respectively. The elution positions of the n = 2–4 γEC peptides were identical with those of the respective peptides purified from *S. pombe*.[11] Amino acid analysis of each peptide gave the expected composition of each and provided the quantitation of peptide concentration. Performic acid oxidation was performed prior to acid hydrolysis in vacuo in 5.7 N HCl. The extent of reduction of cysteinyl thiols was monitored by the dithiodipyridine colorimetric reaction.[23] Peptides were also characterized by automated Edman degradation after alkylation of the cysteinyl thiols with iodoacetate and digestions with carboxypeptidase P[24] and γ-glutamyl transpeptidase.[25] No PTH amino acids were observed in automated Edman degradations of γ-linked peptides, but alternating Glu and CM-Cys were observed in the first eight cycles of Edman degradations of the n = 4 α-analogue followed by Gly in cycle 9. The presence of γ-Glu linkages in the n = 2–4 γ-analogues was verified by incubations with γ-glutamyl transpeptidase followed directly by amino acid analysis. No amino acids were released in the incubation of γ-glutamyl transpeptidase and the n = 4 α-analogue. Carboxypeptidase P is known to cleave all but the γ-linked Glu–Cys bonds in γEC peptides.[24] Incubations of γEC peptides, but not the n = 4 α-analogue, yielded Glu-Cys dipeptides as detected by amino acid analysis. Subsequent incubations of the samples containing dipeptides with γ-glutamyl transpeptidase gave complete hydrolysis of the peptides to individual amino acids. These studies conclusively demonstrate that the isolated peptides were the desired products.

Assays. Peptides in 0.1% TFA were reconstituted with metal ions as described previously (Reese et al., 1988).[8] Metal ions were quantified by atomic absorption spectroscopy on a Perkin-Elmer 305 instrument. Luminescence measurements were conducted on a Perkin-Elmer 650-10S fluorimeter and ultraviolet–visible spectroscopy was performed on a Cary 119 or a Beckman DU-65 spectrometer. Sodium sulfide was titrated into preformed Cd–peptide complexes by using freshly prepared sulfide solutions. Sulfide concentration was quantified with the methylene blue assay.[26] Samples titrated with sodium sulfide were incubated for 16 h prior to sulfide quantitation. This was adequate time for >99% of the sulfide to volatilize in control samples. Photoinduced electron transfer to methyl viologen was performed by mixing Cd–γEC complexes (10 μg of Cd(II)/mL) and 0.2 mM methyl viologen at pH 11.5. The samples were sealed anaerobically and irradiated at 320 nm (20-nm slit) with the xenon source of the Perkin-Elmer fluorimeter.

Results

Properties of CdS Crystallites in Native Isolates. Nanometer-sized semiconductor-type clusters do not exhibit bulk electronic properties due to confinement of electrons and holes in a small volume.[17,18] The carrier confinement results in a size dependency in optical properties and an enhanced redox potential for excited electrons.[27] Native cadmium–sulfide complexes from *C. glabrata* contain a CdS crystallite of nearly 20 Å in diameter coated with approximately 30 n = 2 γEC and n = 2 desGly γEC peptides.[16] Complexes from *S. pombe* contain similar crystallites although a more heterogeneous mixture of particles is apparent.[16] The energy of the near-UV electronic transition (band gap) varies with particle size in clusters less than 100 Å in diameter, which is the size in which bulk semiconductor properties are observed.[19] The energy of this transition in the yeast CdS particles is indicative of particle size.[8,16]

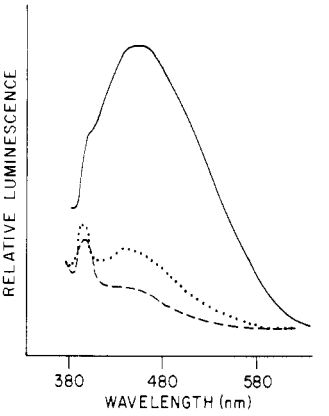

Figure 1. Luminescence of CdS complex from *Candida glabrata*. The sample (S:Cd ratio of 0.62) contained 72 μg of Cd(II)/mL of 20 mM Tris–Cl, pH 7.4, and exhibited a near-UV transition at 313 nm. An emission scan of the native sample (—) was carried out after irradiation at 350 nm. The emission spectra of the sample acidified to pH 1.5 (– –) and subsequently reneutralized to pH 8 (···) were also recorded. After acidification, the S:Cd ratio was reduced to 0.02. The peak at 390 nm is the Raman scatter peak.

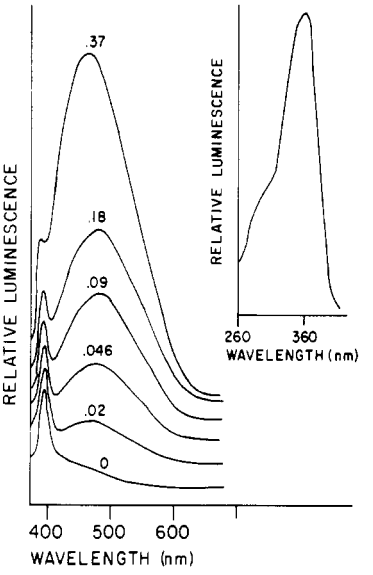

Figure 2. Effect of added sulfide on the emission spectrum of the native CdS complex from *C. glabrata*. Samples (initial S:Cd ratio of 0.5) containing 7.3 μg of Cd(II) were titrated with increasing quantities (molar equivalents) based on the cadmium concentration listed) of sodium sulfide in 0.1 M potassium phosphate, pH 6. After incubation at 5 °C for 16 h, the emission scans were recorded and the remaining sulfide quantified. The sample with 0.37 molar equiv of sulfide added had a final S:Cd ratio of 0.74. The excitation spectrum of this sample is shown in the inset (excitation maximum 360 nm). Emission at 390 nm is due to Raman scattering. Note: the reduced emission in these samples relative to the sample in Figure 1 is a result of the 10-fold lower Cd(II) concentration.

Photoexcitation of synthetic semiconductor clusters is known to result in radiative decay and enhanced photoredox chemistry.[28-30] These reactions are due to poorly understood surface effects.[30,31] Ultraviolet irradiation of the *C. glabrata* CdS cluster (S:Cd ratio 0.6) resulted in luminescence in the visible spectral region (Figure 1). The emission was abolished if the particle was

(22) Sarin, V. K.; Kent, S. B. H.; Tam, J. P.; Merrifield, R. B. *Anal. Biochem.* **1981**, *117*, 147.
(23) Grasseti, D. R.; Murray, J. F. *Arch. Biochem. Biophys.* **1975**, *119*, 41.
(24) Kondo, N.; Isobe, M.; Imai, K.; Goto, T., *Agric. Biol. Chem.* **1985**, *49*, 71.
(25) Anderson, M. E.; Meister, A. *Proc. Natl. Acad. Sci. U.S.A.* **1986**, *83*, 5029.
(26) King, T.; Morris, O. *Methods Enzymol.* **1957**, *10*, 634.
(27) Brus, L. E. *J. Chem. Phys.* **1984**, *80*, 4403.
(28) Chestnoy, N.; Harris, T. D.; Hull, R.; Brus, L. E. *J. Am. Chem. Soc.* **1986**, *90*, 3393.
(29) Nedeljkovic, J. M.; Nenadovic, M. T.; Micic, O. I.; Nozik, A. J. *J. Phys. Chem.* **1986**, *90*, 12.
(30) Henglein, A. *J. Phys. Chem.* **1982**, *86*, 2291.
(31) Brus, L. E. *IEEE J. Quantum Electron.* **1986**, *QE-22*, 1909.

Table I. Effect of Added Sulfide on the Luminescence Emission of the CdS–γEC Complex from *Candidat glabrata*[a]

molar equiv of S added	wavelength max, nm		
	absorbance	excitation	emission
0	304	334	430
0.15	306	339	440
0.3	313	352	455
0.6	317	364	470

[a] Samples containing 112 nmol of Cd(II) present as the native CdS γEC complex (initial S:Cd ratio was 0.5) were titrated with increasing quantities of sodium sulfide in 0.1 M potassium phosphate, pH 7. The absorption, emission, and excitation spectra of the samples were recorded to determine the wavelengths of maximal absorbance and emission.

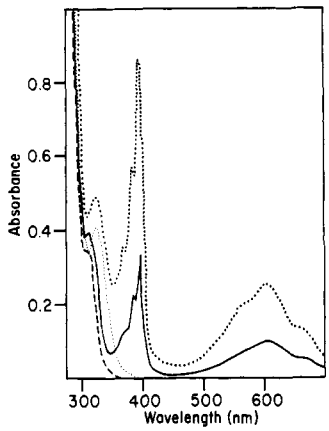

Figure 3. Synthetic and native CdS crystallite-mediated photoreduction of methyl viologen. Anaerobic CdS samples, 10 μg of Cd(II)/mL, isolated from *C. glabrata* were adjusted to pH 11.5 and scanned spectrophotometrically before (--) and after (—) a 10-min irradiation period with a xenon source filtered for 320-nm (20-nm slit) energy. The samples contained 200 μM methyl viologen. The synthetic CdS $n = 2$ complex under similar conditions was scanned before (···) and after (•••) irradiation. The peaks near 375 and 600 are due to the reduced methyl viologen.

acidified to volatilize sulfide ions. Luminescence was accentuated by addition of substoichiometric amounts of sulfide, which facilitates particle accretion (Figure 2).[13] Excess sulfide transiently quenched the emission until the excess had volatilized off. The quantum yield of emission and the wavelength maxima for excitation and emission were dependent on particle size. Samples with a higher S:Cd ratio exhibited red-shifting in electronic transitions, in luminescence excitation maxima, and in emission (Table I). Emission occurred between 430 and 480 nm and excitation between 335 and 370 nm. Emission in sulfide-treated samples was markedly enhanced by substoichiometric quantities of Zn(II) or Cd(II) but quenched by similar quantities of Ni(II) and Cu(II). The surface effect of these ions on the luminescence of low sulfide native complexes was minimal.

Photoexcitation of the *C. glabrata* CdS crystallites in the presence of methyl viologen resulted in the reduction of the dye as monitored by the characteristic absorbance near 600 nm (Figure 3). Accumulation of the reduced dye was dependent on anaerobic irradiation and was enhanced by increasing the CdS particle concentration and by irradiation at alkaline pH's. Samples exhibiting only minimal luminescence were not effective in mediating electron transfer to methyl viologen.

Cadmium–sulfide crystallites coated with different γEC peptides were compared for stability. Native CdS particles from *C. glabrata* and *S. pombe* are heterogeneous first with respect to the length of the γEC peptides and second in particle size as a result of differences in sulfide content.[13] Complexes from *C. glabrata* contain predominantly $n = 2$ γEC and $n = 2$ desGly γEC peptides whereas high sulfide complexes from *S. pombe* contain mainly $n = 3$ and $n = 4$ peptides.[11,20] Native CdS complexes from these fungi were exposed to different conditions to compare stability as measured by the amplitude and wavelength maximum of the

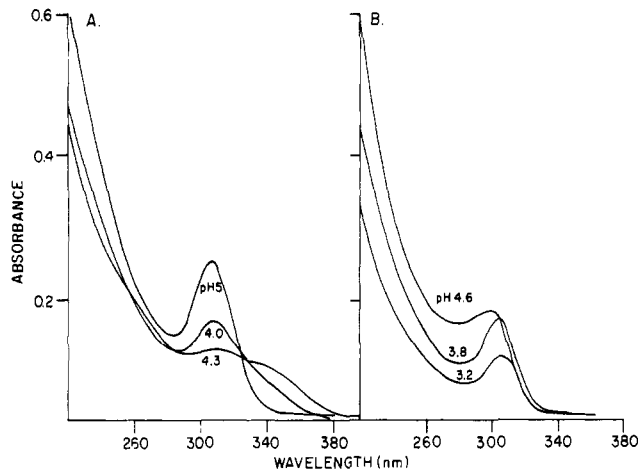

Figure 4. Effect of pH on native CdS crystallites. CdS crystallite samples from *C. glabrata* (panel A) and *S. pombe* (panel B) containing 6.4 and 6.9 μg of Cd(II)/mL of 0.1 M potassium phosphate buffer, respectively, at the pH's listed were scanned for ultraviolet absorption.

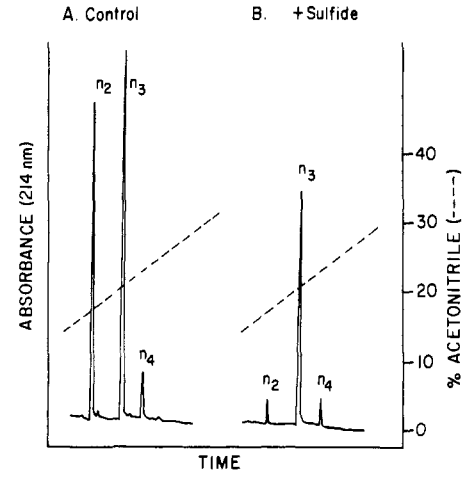

Figure 5. Effect of added sulfide on γEC peptide distribution in CdS crystallites from *S. pombe*. The sample (S:Cd ratio of 0.4) was incubated with 2 molar equiv of sodium sulfide prior to chromatography on Sephadex G-50 equilibrated in 50 mM Tris–Cl, pH 7.6, containing 125 mM KCl. The CdS particles eluted with a higher apparent M_r and contained a final S:Cd ratio of 0.61. Aliquots of the initial sample and final column pool containing 10 μg of Cd(II) were acidified to pH 2 and chromatographed on a C_{18} reverse-phase HPLC column equilibrated in 0.1% trifluoroacetic acid. A linear gradient of 0–60% acetonitrile was used to elute the γEC peptides.

near-UV (band gap) electronic transition.

Native clusters from both species are stable at neutral pH in buffers containing 0–1 M KCl and at low temperatures. Acidification of *C. glabrata* complexes below pH 5 resulted in an attenuation of the near-UV transition and a concomitant red-shifting (Figure 4a). The transition at pH 4 was shifted into the visible spectral region indicative of particle accretion. The resulting CdS particles were readily removed from solution by either 0.2 μm filtration or centrifugation at 12000*g*. In contrast, acidification of *S. pombe* complexes to pH 4 sharpened the electronic transition presumably due to labilization of low sulfide complexes (Figure 4b). Further acidification of this complex attenuated the transition with minimal red-shifting in energies.

CdS particles formed with $n = 2$ γEC peptides were more labile than complexes coated with peptides with a greater number of dipeptide repeats. Addition of sulfide ions to native *S. pombe* Cd–γEC peptide complexes followed by gel filtration resulted in a selective enrichment of $n = 3$ and $n = 4$ peptides at the expense of $n = 2$ γEC peptides originally present in the sample (Figure 5). The displaced $n = 2$ γEC peptides eluted in the internal volume of the column. Likewise, acidification of *C. glabrata* CdS complexes to pH 3 resulted in formation of a sedimentable com-

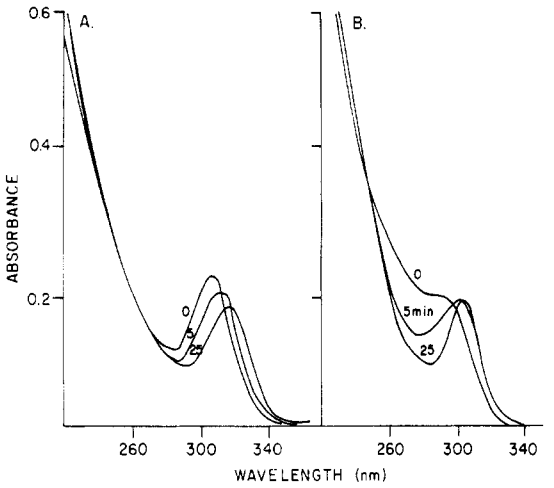

Figure 6. Effect of temperature on native CdS crystallites. CdS crystallite samples from *C. glabrata* (panel A) and *S. pombe* (panel B) containing respectively 6.4 and 6.9 μg of Cd(II)/mL of 0.1 M potassium phosphate, pH 7, were incubated at 65 °C for the times specified, cooled, and scanned for ultraviolet absorption.

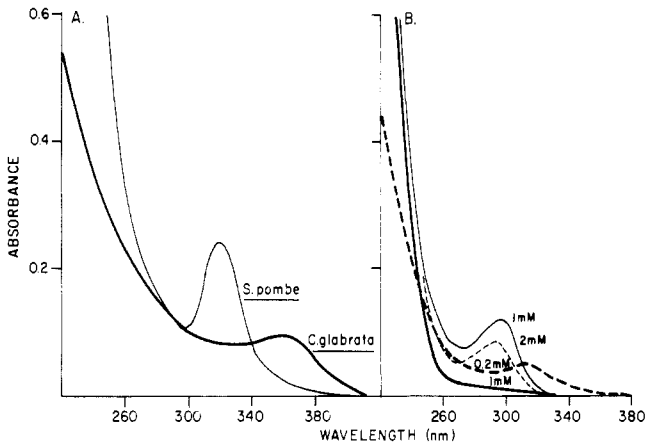

Figure 7. Effect of sulfide and EDTA on native CdS crystallites. CdS crystallite samples from *C. glabrata* (—) and *S. pombe* (—) in 0.1 M potassium phosphate pH 7 were treated with sodium sulfide (panel A) at 1 molar equiv of sulfide based on the cadmium concentration. After 8 h at 23 °C, the absorption spectra were recorded for each. Similar samples were treated with EDTA at concentrations specified, and spectra were recorded after 20 min (panel B).

plex. Evaluation of the γEC peptides by C_{18} reverse-phase HPLC from the acidified sample revealed a selective enrichment of n = 3 peptides in the high sulfide sedimentable complex (n = 2:n = 3 ratio of 3) compared to a preacidification ratio of 6 (data not shown).

Exposure of the native CdS crystallites to elevated temperatures led to a time-dependent red-shifting of the transition in the *C. glabrata* complex to lower energies (Figure 6a). The same temperature caused a sharpening of the transition in the *S. pombe* complex as low sulfide forms of the complex were labilized, but high sulfide complexes were less susceptible to red-shifting in absorbance (Figure 6b). Complexes coated with n = 3 and n = 4 peptides therefore appeared more stable than n = 2 complexes.

Native CdS crystallites were incubated with sodium sulfide to determine the propensity of the clusters to sulfide-mediated particle accretion. Addition of 1 molar equiv sodium sulfide to native *C. glabrata* CdS complexes red-shifted the near-UV transition to over 360 nm (Figure 7a). CdS crystallites having an edge transition near 365 nm are known to be 28 Å in diameter.[16] The sulfide-supplemented *C. glabrata* complex was not removed from solution by filtration or centrifugation (12000*g*). The same quantity of sulfide shifted the spectral transition in native *S. pombe* complexes at pH 7 to only 320 nm, and additional sulfide did not promote any significant shifting beyond this wavelength.

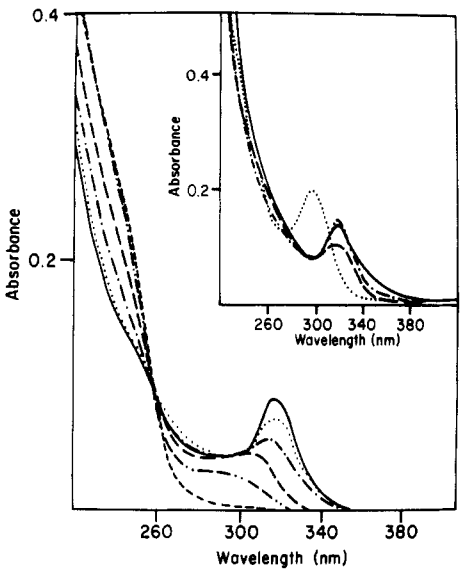

Figure 8. Titration of Cd–γEC n = 3 peptide complex with sodium sulfide. γEC peptide (17.8 nmol) was mixed with 17.8 nmol of Cd(II) at pH 2 followed by neutralization with 0.1 M potassium phosphate, pH 7. Increasing quantities of sodium sulfide were added, and after 16 h at 5 °C, the samples were scanned and quantified for sulfide. Amounts of sulfide added and final S:Cd ratio are as follows: (---) no added sulfide; (-··-) 0.1 mol are equiv, 0.07; (--) 0.2 molar equiv, 0.11; (-·-) 0.4 molar equiv 0.2; (···) 0.8 molar equiv, 0.45; (—) 1.4 molar equiv, 0.57. A final S:Cd ratio of 0.57 was also observed with 2.5 molar equiv of added sulfide. The inset shows samples containing 27 nmol of Cd(II) titrated with 2.5 molar equiv of sulfide at pH 7 in 0.1 M potassium phosphate. Samples include $Cd_{0.5}$ n = 2 (—), Cd n = 3 (-·-), and Cd n = 4 (--) γEC peptides and $Cd_{1.5}$ n = 4 α-peptide (···). Final S:Cd ratios for these samples were 0.76, 0.56, 0.51, and 0.62 respectively.

Native CdS complexes coated with γEC peptides are labile to chelators such as EDTA. The near-UV electronic transition was abolished in crystallites from *C. glabrata* upon treatment with 1 mM EDTA, whereas the band gap transition in *S. pombe* was largely unaffected (Figure 7b). Addition of 2 mM EDTA attenuated the transitions of the latter complexes.

Crystallites Formed in Vitro with γEC Peptides. Metal ions associated with γEC peptides in vitro in the absence of sulfide ions. Binding stoichiometry for Cd(II) ions was determined by monitoring the absorption spectra of peptide samples reconstituted with increased molar equivalents of Cd(II). The absorbance in the ultraviolet is dominated by metal–thiolate charge-transfer transitions. The molar equivalency yielding maximal absorbance at 250 nm was near 0.5, 1, and 1 for n = 2–4 γEC peptides, respectively. These stoichiometries were used for subsequent studies.

Cadmium complexes with γEC peptides were titrated at pH 7.0 with sulfide ions to study the in vitro assembly of CdS crystallites. Titration of Cd n = 3 peptide complexes with an increasing quantity of sodium sulfide resulted in a maximal S:Cd ratio of 0.57 within the complex and an electronic transition maximally red-shifted to 318 nm (Figure 8). Transitions were blue-shifted at lower S:Cd ratios. Cadmium–sulfide complexes formed with half the maximal Cd(II) stoichiometry also showed near-UV transitions of similar energies but attenuated in intensity. Titrations of other Cd–γEC peptide complexes with 2.5 molar equiv of sodium sulfide yielded near-UV electronic transitions near 318 nm for each CdS–γEC complex (Figure 8, inset). Formation of the CdS n = 2 complex with excess sulfide yielded greater absorbance at wavelengths above 318 nm, consistent with some sulfide-mediated accretion.

Formation of CdS particles as a function of pH showed that the near-UV electronic transition was blue-shifted with increasing pH. The magnitude of the shift was more pronounced for n = 3 and n = 4 γEC complexes compared to n = 2 complexes (Figure 9). The quantity of sulfide incorporated within the complex decreased with increasing pH. The final S:Cd ratios for n = 2

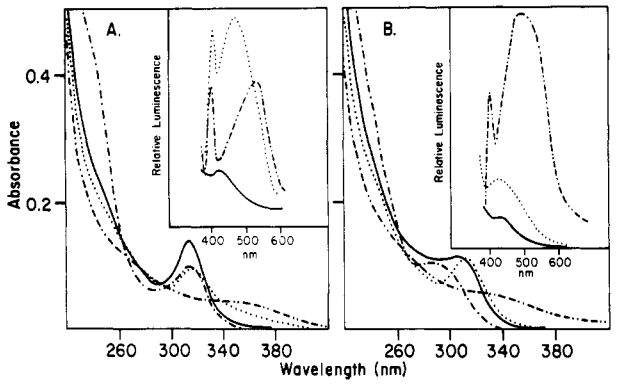

Figure 9. Effect of pH on formation of CdS crystallites in vitro with n = 2 (panel A) and n = 3 (panel B) γEC peptides. Cd(II) peptide complexes at stoichiometries and concentrations listed in the legend to Figure 7 were neutralized with 0.1 phosphate at varying pH's and incubated with 1 molar equiv of sodium sulfide. The samples were scanned for ultraviolet absorption. The following pH's were used: (-··-) pH 5; pH 6 (···), (—) pH 7; (-·-) pH 9. The inset shows the emission spectra of the samples at pH 5, 6, and 7 with similar lines as mentioned specifying pH. The wavelength of maximal excitation was used in each case. These wavelengths include 368, 368, and 330 nm for the pH 5, 6, and 7 n = 2 samples, respectively, and 360, 330, and 330 nm for the pH 5, 6, and 7 n = 3 samples, respectively.

and n = 3 complexes at pH 9 were 0.38 and 0.32, respectively. Despite similar S:Cd ratios at pH 9, complexes with n = 3 were blue-shifted from 315 nm, whereas n = 2 complexes showed marked reduction in the intensity of the near-UV transition. Formation of the CdS complex with each peptide at pH values below 6 resulted in some bulk CdS formation based on absorption spectroscopy, the amount of these highly red-shifted species declining with increasing peptide length (Figure 9).

CdS complexes formed in vitro exhibited luminescence. Emission with the CdS n = 2 and n = 3 samples at pH 7 was maximal at 420 and 430 nm with excitation maxima of 330 and 335 nm respectively. The emission yield varied with the pH with maximal emission occurring with the CdS n = 2 compound at pH 6.0 and the CdS n = 3 compound at pH 5.0 (Figure 9, inset). The increased emission in the complexes correlated with the greater red-shifting in the near-UV transition in sulfide-titrated samples. Addition of Zn(II) ions to the sulfide-treated samples enhanced the emission as in native complexes. The samples formed in vitro were also competent in mediating the photoinduced reduction of methyl viologen (Figure 3). These properties verified that Cd binding to γEC peptides nucleated CdS crystallites growth in a manner analogous to growth of particles formed in vivo.

CdS Particle Formation with Non-γEC Peptides. Cysteine-containing peptides with α-peptide bonds were compared for their ability to coat CdS crystallites. Peptides of the n = 4 and α type a mouse metallothionein hexapeptide (Lys-Cys-Thir-Cys-Cys-Ala) were used. Initial titrations of Cd(II) ions with these two peptides demonstrated maximal binding stoichiometries of 1.5 and 0.9 for the n = 4 α-peptide and the MT hexapeptide, respectively. Cd–peptide complexes were titrated with increasing amounts of sulfide, and the absorption spectra were recorded. Addition of sulfide to the MT hexapeptide led to a red-shifting of the near-UV transition, becoming a maximum at an energy corresponding to 295 nm. Excess sulfide did not further affect the energy of this transition at pH 7. The maximal S:Cd ratio of samples titrated with sulfide was 0.45. Luminescence was observed at 450 nm with hexapeptide samples only at pH 5, a pH in which the near-UV transition was broadened to over 340 nm. The formation of the CdS–hexapeptide complexes occurred at pH values between 6 and 8 and at Cd:hexapeptide stoichiometries below 0.9.

Results with the n = 4 α-peptide were comparable to those with the MT hexapeptide. CdS particle formation readily occurred between pH 5 and 9, but the near-UV electronic transition became maximally shifted near 300 nm unlike the maximal 320-nm transition for the n = 4 γ-peptide (Figure 8 inset). Although the α-peitde forms complexes with higher energy transitions than the γ-peptide, the S:Cd ratios are respectively 0.62 and 0.51. This is in opposition to results with γEC peptides in which the energy of the near-UV transition is related to the sulfide content of the cluster. Despite the differences in sulfide content, CdS complexes formed with γEC and αEC peptides exhibited a similar Stokes' radius on gel filtration (data not shown). The CdS αEC complex was luminescent, but emission was minimal compared to that for CdS γEC n = 4 complexes.

Discussion

Nanometer-sized CdS crystallites are formed in *C. glabrata* and *S. pombe* in response to cultures containing cadmium salts.[16] A heterogeneous mixture of short isopeptides coats the crystallites. Formation of the small particles appears to be a matrix-mediated mineralization process, dependent on γEC peptides. This is a common pathway of intracellular biomineralization.[32,33] The γEC-peptide-mediated biomineralization is not unique to fungi. The process can be mimicked in vitro with Cd–γEC peptide complexes and other cysteine thiolate-containing peptides. CdS crystallite formation is controlled in fungi by Cd(II)-regulated concentrations of γEC peptides and sulfide. Cd(II) binding to γEC peptides appears to provide the matrix for the sulfide-driven biomineralization. The initial Cd–peptide complex appears to be an oligomer of multiple peptide units stabilizing a Cd–thiolate polynuclear cluster.[4,9] The size of the CdS crystallite is dependent first on the magnitude of the Cd(II)-stimulated sulfide generation in the cells and second on the ability of γEC peptides to stabilize discrete sizes of particles. The particular lattice size and stability of the particles are dictated by the coating peptides. γEC peptides from n = 2 to n = 4 preferentially stabilize particles near 20 Å in diameter. The CdS particle isolated from *C. glabrata* was calculated to contain a lattice of 85 CdS units sheathed with nearly 30 γEC peptides.[16] Peptides of αEC and the MT hexapeptide stabilize crystallites with higher energy band gap transitions than clusters formed with γEC peptides. This difference between peptide coats may relate to different lattice sizes or to different mineral lattice structures. Cadmium sulfide can form crystal lattices as three distinct minerals including zinc blende, wurtzite, and, under high pressure, rock salt. The Bragg diffraction pattern of CdS complexes from *S. pombe* and *C. glabrata* was not conclusive in assigning a lattice structure[16] and is being reevaluated. The short coherence length in the crystallites limits the resolution between diffraction patterns of model CdS mineral lattices.

The particles are dynamic in that particle accretion occurs with larger particles forming at the expense of smaller ones. This process, known as Ostwald ripening, is a well-characterized phenomenon with small metal crystallites.[17] The accretion process occurs at room temperature and neutral pH only with prolonged incubation but is facilitated at elevated temperatures or acidic pH. Partial uncoating or incomplete coating of the particle is presumably necessary for accretion. Particles coated with γEC peptides with more than two dipeptide repeats are more stable against this particle coalescence. The length effect is probably related to a multidentate effect of multiple cysteinyl thiolates within the peptide. The increased tethering with increased number of cysteinyl residues may reduce the probability of uncoating of the crystallite. An alternative explanation is that CdS crystallites are more solvent exposed when coated with n = 2 γEC peptides compared to longer peptides. Sulfide ions but not Cd(II) ions also facilitate particle aggregation. This accretion may occur by virtue of a cross-linking effect of sulfide anion of adjacent particles or a facilitated uncoating by competition binding with cysteinyl thiolates.

The enhanced stability of Cd(II) complexes with n = 3 and n = 4 γEC peptides may explain the reduced effectiveness of these peptides as a matrix for CdS mineralization. Since these complexes function in metal ion detoxification, stability and ease of complex formation are critical factors. Efficiency of detoxification is expected to be enhanced by optimizing both stability and

(32) Lowenstam, H. A. *Science* **1981**, *211*, 1126.
(33) Mann, S. *Nature* **1988**, *332*, 119.

formation. Such optimization may have been the selective pressure for the predominance of $n = 2$–4 γEC peptides in nature. Peptides of the $n = 1$ type (glutathione) will serve as a matrix for CdS formation, but stability is low and GSH-coated particles show facile accretion.[34] Cd(II) complexes with γEC peptides longer than $n = 4$ are predicted to be less effective in nucleating CdS crystallite formation perhaps by virtue of enhanced stability of Cd–cysteinyl thiolate clusters. The importance of sulfide in metal detoxification is highlighted by the isolation of sulfide-deficient *S. pombe* mutants that exhibit cadmium hypersensitivity.[15]

The increased stability of *S. pombe* CdS crystallites does not imply that *S. pombe* is more resistant to cadmium salts than *C. glabrata*. The yeast *C. glabrata* is highly resistant to toxicity of cadmium salts. Formation of CdS crystallites is only one cellular detoxification mechanism in this organism. The other mechanisms have not been elucidated.

The crystallites exhibit properties analogous to those of semiconductor clusters. The yeast CdS particles are quantum crystallites that luminesce and mediate electron transfer to methyl viologen. The latter two properties are attributed to the localization of excited electrons on the surface of the particles.[31] Luminescence in synthetic CdS semiconductor clusters is attributed to the recombination of a photogenerated electron and an existing hole.[28] The electronic state of the electron is not apparent in the absorption spectrum.[28] Luminescence correlates with particle size and is influenced by surface adsorbed cations. Cations are known to quenched the luminescence of synthetic colloidal CdS.[30] The effect is attributed to electron scavenging at the surface of the particles. Electrons are also scavenged by methyl viologen at the surface. Under anaerobic conditions, the reduced dye is stable against facile oxidation, but a significant back-reaction occurs that is attributed to reoxidation of the dye by trapped holes (h+) in the particle.[30] The presence of hole scavengers has been shown to inhibit this route of oxidation in some but not all studies.[35,36] Crystallites formed in vitro with γEC peptides exhibit corresponding excited electronic state properties.

The effectiveness of γEC peptides in stabilizing discrete sizes of CdS crystallites either in vivo or in vitro may enable the peptides to be used as a matrix for other types of mineralization where discrete particle size is desired. As metal–sulfide clusters are used as photosensitizing and catalytic agents,[30,37] discrete sizes of these quantum particles may yield more predictable properties. Presently, synthetic semiconductor clusters are typically coated with nonspecific organic polymers, leading to a wide spectrum of particle sizes.

Acknowledgment. We acknowledge the support by National Institutes of Health Grants ES 03817 and ES 00147 to D.R.W. and Training Grant T32 AM 07115 to C.T.D. We also thank Drs. R. K. Mehra and R. N. Reese for helpful discussions and Dr. W. R. Gray for assistance in peptide synthesis.

(34) Dameron, C. T.; Winge, D. R. *J. Biol. Chem.*, in press.

(35) Gratzel, M. *Acc. Chem. Res.* **1981**, *14*, 376.
(36) Kuczynski, J.; Thomas, J. K. *Langmuir* **1985**, *1*, 158.
(37) Kuczynski, J.; Thomas, J. K. *Chem. Phys. Lett.* **1982**, *88*, 445.

Contribution from the Department of Chemistry, Massachusetts Institute of Technology, Cambridge, Massachusetts 02139, and Department of Radiology, Harvard Medical School and Brigham and Women's Hospital, Boston, Massachusetts 02115

Technetium Nitrido Complexes with Amine and Thiolate Ligands: Structural Characterization of $TcN(SC_6HMe_4)_2(NHC(NMe_2)_2)_2$, a Complex with Coordinatively Bound 1,1,2,2-Tetramethylguanidine

Nadine de Vries,[1a] Catherine E. Costello,[1a] Alun G. Jones,[1b] and Alan Davison*[,1a]

Received June 19, 1989

A methanol solution of the Tc(VI) complex $(Ph_4As)[TcNCl_4]$ is reduced in the presence of pyridine to give the orange Tc(V) complex $[TcN(OH)(py)_4](Ph_4B)$ (**1**). As in the oxo analogue $[TcO_2(py)_4](Ph_4B)$, the pyridine ligands on **1** are labile and undergo exchange with free pyridine in solution. The TcO_2^+ and $TcN(OH)^+$ cores also appear to be similar electronically, since the ^{99}Tc NMR chemical shifts for these two compounds are not significantly different. Compound **1** reacts with 2,3,5,6-tetramethylbenzenethiolate (tmbt) to give quantitative yields of the robust compound *trans*-$TcN(tmbt)_2(py)_2$ (**2**). In an attempt to prepare $[TcN(tmbt)_4]^-$, $[TcNCl_4]^-$ was allowed to react with Htmbt in the presence of the "noncoordinating" base 1,1,3,3-tetramethylguanidine (TMG). Instead of the desired tetrathiolate complex, $TcN(tmbt)_2(TMG)_2$ (**3**), a rare example of TMG coordination, was obtained. This compound shows dimer formation in fast atom bombardment spectra, and the decomposition of this species was studied by tandem mass spectrometry. The structure of **3** was confirmed by a single-crystal X-ray structure determination (crystal data: molecular formula = $C_{30}H_{52}N_7S_3Tc$, monoclinic, $a = 9.006$ (3) Å, $b = 24.815$ (3) Å, $c = 15.992$ (2) Å, $\beta = 96.57$ (2)°, space group = $P2_1/n$, $Z = 4$, final $R = 0.048$, final $R_w = 0.057$).

The nitrido and oxo groups are isoelectronic,[2] but despite the large number of oxotechnetium compounds known, few nitrido compounds were reported until recently. In 1981, Baldas et al. reported the preparation and crystallographic characterization of the first technetium nitrido complex, $TcN(S_2CNEt_2)_2$.[3] Soon after, the same authors reported the synthesis of $(Ph_4As)[TcNCl_4]$,[4] a convenient starting material for the further exploration of complexes containing the Tc≡N bond. This complex has been shown to undergo ligand exchange and yield products in which displacement of chlorides is accompanied by a one-electron reduction of the metal. Part of the current effort in exploring technetium nitrido complexes is directed toward the preparation of the nitrido analogues of oxo compounds, which have proven useful in diagnostic nuclear medicine.[3,5]

We have recently explored the chemistry of oxotechnetium(V) complexes with sterically hindered arenethiolate ligands. Reaction of $(n\text{-}Bu_4N)[TcOCl_4]$ with 2,3,5,6-tetramethylbenzenethiolate (tmbt) yields the five-coordinate anionic species $(n\text{-}Bu_4N)[Tc(tmbt)_4]$.[6,7] When the reaction is performed in the presence of

(1) (a) Massachusetts Institute of Technology. (b) Harvard Medical School.
(2) Griffith, W. P. *Coord. Chem. Rev.* **1972**, *8*, 369.
(3) Baldas, J.; Bonnyman, J.; Pojer, P. M.; Williams, G. A.; Mackay, M. F. *J. Chem. Soc., Dalton Trans.* **1981**, 1798.
(4) Baldas, J.; Boas, J. F.; Bonnyman, J.; Williams, G. A. *J. Chem. Soc., Dalton Trans.* **1984**, 2395.
(5) Baldas, J.; Bonnyman, J. *Int. J. Appl. Radiat. Isot.* **1985**, *36*, 919.
(6) Davison, A.; de Vries, N.; Dewan, J. C.; Jones, A. G. *Inorg. Chim. Acta* **1986**, *120*, L15.

0020-1669/90/1329-1348$02.50/0